15th IFK
Proc. of the 15th International Fluid Power Conference <Symposium/Conferenc

Model-Based Valve Design: Potential of CFD Simulations as a Database for Prediction Models

Timo Rothhardt, Jakob Wirtz, Katharina Schmitz

RWTH Aachen University – Institute for Fluid Power Drives and Systems (ifas), timo.rothhardt@ifas.rwth-aachen.de, sc@ifas.rwth-aachen.de

Abstract.

Conventional valve development includes measurements and computational fluid dynamics (CFD) simulations. Both are used in an iterative process to achieve the desired characteristic curve. To accelerate the valve development process considerably, data-based expert systems should be introduced. These models are trained with CFD simulation data of numerous geometries. Usually, CFD simulation parameters are tuned for one specific geometry.

This paper presents CFD simulation parameters applicable for a wide range of 2/2 directional poppet valve geometries. The parameters are validated with measurement data from both normally open (NO) and normally closed (NC) valves. Based on previous research, the theoretical background in CFD simulation and preliminary studies, the simulation parameters used in this study are carefully selected. For the validation, 164 points are generated from continuous measurements of nine industrial poppet valves. The comparison between the simulations and measurements show a very high accuracy in the prediction of the pressure difference with a mean deviation of 7.9 %. The accuracy in the simulation of flow forces is lower but the trends in the simulations are correct and high flow forces can be predicted accurately. The results prove that it is possible to use one set of CFD simulation parameters for different geometries. This makes CFD simulations suitable as a database for prediction models.

Keywords. Model-based valve design, poppet valves, flow forces, CFD simulation, validation.

1. INTRODUCTION

Oil hydraulic valves are used in a wide range of industrial and mobile hydraulic applications for simple switching functions as well as for control tasks. The variants within a valve series are often as diverse as the applications themselves. Nevertheless, there are always customer requirements that call for a further, adapted valve geometry. Being able to implement these requirements quickly and cost-effectively plays a decisive role in global competition.

Currently, developing valves for specific applications is time-consuming and costly. This is because valve development is an iterative process involving trials and CFD simulations, which requires expert knowledge and is usually based on the experience of individual company employees. Demographic change and a changing work environment with higher job fluctuation among employees requires knowledge to be documented and formalized [1]. In a recent study by PwC, almost three quarters of all respondents expect personnel costs to rise by 4.7 % in 2026 and see the shortage of skilled workers and increasing cost pressure as obstacles for corporate growth [2].

These challenges can be addressed with an innovation of the development process. So called expert systems can represent complex relationships in an easy-to-use single model. Such a model can calculate the same correlations in a few seconds with the same accuracy. An expert system for valve development could allow the user to define a customer-specific characteristic flow curve, which the system uses to calculate the optimum valve geometry.

To make this step, there is a lack of fast calculating models that can be inverted. Measurements take long but are still the most exact way to determine pressure losses and flow forces. CFD simulations are faster but a little less accurate [3]. Analytical equations are fast to calculate and invertible but not as exact, especially in the determination of flow forces [4].

The solution is a data-based approach, where data is collected and metamodels are trained. As such, CFD simulations should be used as the database, since geometries are easy to manipulate and data is easily gained across a wide range of geometries. When simulating hundreds of different geometries, it is not possible to tune the simulation parameters for each geometry. Thus, generally applicable CFD simulation settings are needed.

This paper presents the selection and validation of generally applicable CFD simulation parameters for 2/2 directional poppet valves with nominal flow rates from 20 l/min to 40 l/min. To determine optimal parameters, at first, previous research about CFD simulations of poppet valves is elucidated and a detailed review of CFD simulation parameters as well as their influence is given. The next chapter outlines the conducted simulations. The selection of points for simulation from continuous measurement data is explained, the preliminary studies on CFD simulation parameters presented and the methodology for the simulation of numerous operating points described. In the last chapter, the simulation results are compared to measurement data, and the accuracy of the simulations is discussed and improved.

2. FUNDAMENTALS

This chapter presents previous research about the CFD simulation of flow forces in poppet valves and gives an overview about the most important CFD simulation parameters and their influence on the simulation model. The focus of the reviewed literature lies on the flow forces and not the pressure difference since it is more challenging to achieve a high accuracy in the CFD simulation of flow forces [3]. The aim is to identify commonly used CFD simulation parameters as a basis for this study. For the flow forces, the convention used is that a positive flow force acts in the closing direction. The detailed definition and an example cross-sectional view of a valve with labelled ports are provided in [5].

2.1. Simulation-based Analysis of Flow Forces in Poppet Valves

The numerical simulation of flows in poppet valves started in the early 90s. Especially in the beginning, the focus was to show that simulated flow patterns equal the flow patterns from measurements [6]. Recent research focusses on improving the accuracy of CFD simulations by implementing new models (e.g. turbulence or cavitation models) or optimizing components by varying selected geometrical parameters. In the optimization of valves, the pressure drop and the flow induced forces on the poppet are the most relevant quantities. Investigations show that the simulation of the flow forces is more inaccurate than the simulation of the pressure drop [7]. Particularly for the numerical simulation of flow forces, there is no generally valid combination of simulation parameters (e.g. mesh type, mesh size and turbulence model) for accurate results [3]. Zong et al. [8] show that the turbulence model has a strong influence on the results of the simulated flow force while the pressure drop was nearly unchanged. Therefore, the focus of this chapter lies on previous research that simulated flow forces in poppet valves and the employed simulation parameters. Due to large steps in CFD modelling and computing power in the last years, only recent research from 2010 and later is considered. Not all CFD simulation parameters are mentioned in the following brief content description of the papers but summarized afterwards in a table.

Domagala and Fabis-Domagala [9] published a detailed review of research about the CFD simulation of flow forces in both spool and poppet valves. The paper covers the theoretical background of flow forces in valves and of CFD methods as well as numerous publications about steady-state and transient flow simulations. The review results in commonly used assumptions in the CFD simulation of flow forces:

- The fluid is homogeneous, single-phase, incompressible and has constant properties.
- All valve geometries are ideal.
- The roughness of components is neglected, and walls are modelled as smooth.
- Heat transfer and phase changed are neglected.
- The turbulence models used are a standard k-ε or RNG k-ε

Bernad and Susan-Resiga [10] use a 2D CFD simulation to investigate cavitation in a highly simplified seat valve. The fluid is modelled as multi-phase and the main dynamics of the cavitating flow can be mapped. Hao et al. [11] examine three simple cone geometries in a water valve with the aim of reducing flow forces and cavitation in the valve. Steady-state 2D CFD simulations are performed with a two-phase (water and steam) mixture. On the third valve, two housing parameters at the valve outlet are varied individually. By combining the optimal parameters, the flow force is reduced by 44.2 %. Simic and Herakovic [12], [13] optimize the geometry of a normally closed (NC) valve geometry with the aim of reducing flow forces in static operation. The influence of five geometric parameters on the flow forces is investigated by using 3D CFD simulations. For one parameter, additional experiments confirm the accuracy of the CFD simulations with a maximum deviation of 7 %. Xie et al. [14] and Liu et al. [15] investigate basic cone geometries and vary different geometrical parameters in 3D CFD simulations. The method one-factor-at-a-time (OFAT) is used by both authors and the influence of the parameter changes on the flow forces are evaluated.

Rundo and Altare [16] compare two analytical flow force models (Bernoulli and momentum conservation) with stationary CFD simulations. Both flow directions and three poppet angles are considered. In flow direction 1-2, the analytical calculation according to Bernoulli achieves similar results to the CFD simulation, while in direction 2-1, Bernoulli calculates a flow force that is seven times greater. This shows that physical models are not well suited for the analytical calculation of flow forces. Roemer et al. [17] develop their own analytical model for calculating the forces on the poppet of a fast-acting valve. This model considers flow-induced and motion-induced forces. The parameters for the analytical model are determined using a series of transient CFD simulations, which means that a one-time high simulation effort is required to obtain the analytical model.

Transient CFD simulations are used by Gomez et al. [18] to investigate the dynamics of a commercially available valve. In the simulations, the switching frequencies, inlet pressures and poppet angles of the valve are varied, and the pressure loss and flow force are evaluated. The poppet angle has little effect on pressure loss and mainly affects the flow force. Finesso and Rundo [19] develop a transient simulation of a pressure relief valve to predict the valve characteristics for different geometries and spring settings. The CFD simulation is validated with measurements and shows good agreement. Based on few CFD simulations, a 0D model is tuned and can predict the flow characteristics of the valve. Hirose et al. [20] use transient 3D CFD simulation to investigate the force hysteresis induced by flow patterns on the valve poppet. In preliminary steady-state simulations, the flow patterns described by Johnston et al. [21] are confirmed by simulation. The transient simulations show that the change in flow pattern occurs at different positions when the valve is opened and closed. All CFD simulation parameters mentioned in the presented papers, are summarized in **Table 2.1**. The properties not mentioned are marked with [-].

Author	**2D or 3D Steady-state or transient**	**Turbulence model**	**Fluid model (Fluid specification / fluid phases / cavitation)**	**Discretization scheme (pressure / momentum / k / ε or ω)**
[10]	2D Steady-state	RNG k-ε	[-], two-phase, cavitation	SIMPLE / second-order / first-order / first-order
[11]	2D Steady-state	Realizable k-ε	Water, two-phase, cavitation	PRESTO! / second-order / second-order / [-]
[12]	3D Steady-state	k-ω SST	Oil VG 32, single-phase, [-]	[-]
[13]	3D Steady-state	k-ω SST	Oil VG 32, single-phase, [-]	[-]
[14]	3D Steady-state	k-ε	[-]	[-]
[15]	3D Steady-state	RNG k-ε	Density and viscosity, [-], [-]	[-]
[16]	3D Steady-State	k-ε	Oil, two-phase, cavitation	First-order upwind
[17]	3D Steady-state and transient	Laminar flow	Oil, single-phase, [-]	[-]
[18]	3D Transient	k-ε	Oil VG 32, single-phase, [-]	SIMPLE / second-order / second-order / second-order
[19]	3D Transient	k-ε	Oil DTE 25, two-phase, cavitation	PRESTO! / QUICK / first-order / first-order
[20]	3D Steady-state and transient	k-ε	Density and viscosity, [-], [-]	[-]

Table 2.1: Overview of CFD simulation parameters used in previous investigations

Based on the overview in the table it can be said that most of the simulations of poppet valves in the last years were 3D CFD simulations. Depending on the research objective, both steady-state and transient simulations were set up. The most used turbulence model was, as described by [9], some kind of k-ε model. Some publications name the fluid with the operating temperature and the resulting density and viscosity; others name only the density and viscosity or do not name any fluid properties. The discretization schemes used differ between the investigations, but for the momentum the second-order upwind scheme is the most common. The most commonly used simulation environment is Ansys® Fluent® and the mesh type an unstructured tetrahedron-mesh.

2.2. *Simulation Parameters and Their Influence*

The construction process of a CFD simulation entails a wide range of choices and parameters that require careful consideration and are essential for its success. This section will provide an overview of crucial decisions during the setup process of a typical CFD simulation in Ansys® Fluent®. The general workflow for a CFD simulation first involves the conception of a geometry which is then discretized into a mesh and finally examined by a CFD solver. The geometry is usually created with a CAD software and then imported into the CFD environment. Therefore, the focus of the simulation parameters lies on the mesh and solution settings. Mesh creation and numerical simulation in general is always a balancing act between accuracy and computational cost.

2.2.1. Mesh

Meshes can be categorized into two main mesh types – structured and unstructured meshes. In structured meshes the cell coordinates align with the cartesian coordinates and a cell always has a predefined number of neighbours. The structured grid is limited to simple geometries because both complex walls and tight spaces, that require the use of a finer mesh, would introduce unnecessarily small spacings in other parts of the solution domain in order to maintain the structured nature [22]. Structured meshes also minimize the effects of numerical diffusion when using the first-order upwind scheme for cell discretization, because the second-order derivatives from the Taylor series expansion, that cause numerical diffusion, are ideally one-dimensional when the flow is aligned with the grid [23].

Unstructured meshes are able to fit an arbitrary solution domain and are thus the most flexible of all grid types when it comes to meshing irregular geometries. They are not limited by the number of cell neighbours and allow for all types of cell shapes, including tetrahedrons or polyhedrons in three dimensions. This type of mesh involves a computational overhead during construction due to its arbitrary nature and lack of simple indexing system [24]. It also requires more complex methods for gradient computation as it is not able to rely on cartesian directions and is additionally very vulnerable to numerical diffusion when using first-order upwind schemes for cell discretization [25]. Despite these challenges, unstructured meshes have become increasingly popular and there are several methods to alleviate the drawbacks, as will be elaborated upon in chapter 3.2. Comparing tetrahedron- and polyhedron-meshes, polyhedron-meshes require more computation time during the mesh generation. This overhead is compensated, however, in the total computation time of the solution due to a lower overall cell count [24].

In all cases, when flow becomes oblique to the grid cells or is characterized by high gradients, the solution is prone to discretization errors [22]. Said errors are proportional to the truncation errors from the Taylor series expansion of the used discretization schemes. In the case of this first-order upwind scheme, the leading error term is a second derivative which corresponds to the mathematical description of physical diffusion. The truncation error thus adds a diffusion term to the solution making it overly diffusive. This effect is commonly referred to as numerical or false diffusion. A reduction of the overall spatial discretization error can be achieved by reducing the cell size or by the choice of the discretization scheme. Important differences are between the first- and second-order upwind scheme, because the first-order scheme introduces numerical diffusion effects, as previously explained, whilst the latter alleviates these effects by eliminating the second derivative in the truncation error [25].

Furthermore, it is important to appreciate that over-refining the mesh across the entire solution domain does not necessarily improve the overall results. Convergence of the solution depends on the residuals of the discretized conservation equations throughout the entire domain. When determining the appropriate mesh size and refinement regions, it is thus important to attempt a balance in the discretization error across the entire domain, namely a similar residual in all domain parts [22].

Finally, the design of a meaningful mesh requires the consideration of near-wall effects, in particular the adequate resolution of the viscous sublayer and buffer layer. To achieve this, meshes are typically either equipped with boundary-layer elements or with wall functions. Boundary layers essentially provide fine resolution in the wall-normal direction. In this way, near-wall effects can be represented accurately with only a modest increase in computational cost. Wall functions are semi-empirical formulas that interpolate the viscous sublayer and buffer layer, omitting the necessity of a complete resolution of the near-wall region [25].

2.2.2. Solution

This section focusses on the interpretation of the mesh in terms of discretized conservation equations and also endeavour to elucidate relevant decisions during turbulence modelling. Before beginning any type of solution, it should first be examined what kind of characteristics the flow is expected to have; strictly laminar or turbulent. If the flow is strictly laminar, the underlying conservation-equations are usually solved using any type of numerical solver. If the flow is presumed to assume turbulent characteristics at some point in the domain, the solution complexity increases drastically. The numerical examination of turbulent flow can generally be categorized into three types of simulation: the direct numerical simulation (DNS), the large-eddy simulation (LES) and the Reynolds-averaged Navier-Stokes (RANS)-approach [22].

The DNS is the most exact approach for turbulent simulations but entails significant computational cost. LES is a compromise between computational cost and accuracy. It is usually used in cases where the DNS is too computationally expensive like in high-Reynolds flows or for complex geometries. The RANS-approach is the least computationally expensive and entails the replacement of flow variables in the conventional Navier-Stokes equations by quantities that underwent Reynolds-averaging, namely the separation of flow variables into an averaged and a fluctuating quantity. During this averaging process an additional unknown quantity emerges called the Reynolds stress tensor (RST). This tensor can be approximated with the help of the turbulent kinetic viscosity which, in return, is then modelled with additional equations [22].

Said modelling can be implemented in the form of zero-, one- or even six-equation models, the most common, however, being the two-equation model. In the realm of two-equation-models, the most prominent are the k-ε and the k-ω models. Both cases institute two transport equations, one for the turbulent kinetic energy k and one for either the dissipation rate of k, namely ε, or the specific dissipation rate of k, namely $\omega = \varepsilon/k$. The k-ε is very popular in general industrial CFD applications because it provides reasonable accuracy for a wide range of simulation problems. However, it is not integrable through the viscous sublayer without the addition of further equations, limiting its accuracy in the prediction of near-wall phenomena. The k-ω model addresses this limitation and is conceived in a way that allows it to adequately predict the viscous sublayer, making it the better choice for simulations involving extensive wall-modelling [25].

3. CFD Simulations

The CFD simulation parameters should be validated based on the measurements of 9 poppet valves. Due to the measurement procedure with a moving poppet, required to capture the flow forces, the measurement data is continuous [5]. At first, this chapter shows how discrete points for CFD simulation are extracted from the continuous measurement data. Since generally applicable CFD simulation settings are needed, preliminary studies are conducted to determine most of the CFD simulation parameters. Finally, the methodology and procedure for the batch simulation of different valve geometries with different opening widths and boundary conditions are described briefly.

3.1. Determining the Point of Operation

The simulated points of operation should be as close as possible to the real point of operation. How the point of operation is determined, differs between NO und NC valves. For NO valves, the actual operating point can be easily read from the measurement data. It is the point at which the rod of the valve actuation and force measurement system lifts off the poppet. At this position, there is a balance of forces at the poppet between the flow force acting in the closing direction and the spring force acting in the opening direction. The measurements in [5] were conducted with different tank pressures and pressure differences over the valve.

Figure 3.1 shows the poppet position x, the flow rate Q and the measured force F plotted over time t for one cycle of a NO valve. The actual operating point is located at the position where these variables begin to change with the poppet position, since this is the point where the rod of the through-drive starts touching the poppet. From this point on, the measured position also corresponds to the poppet position.

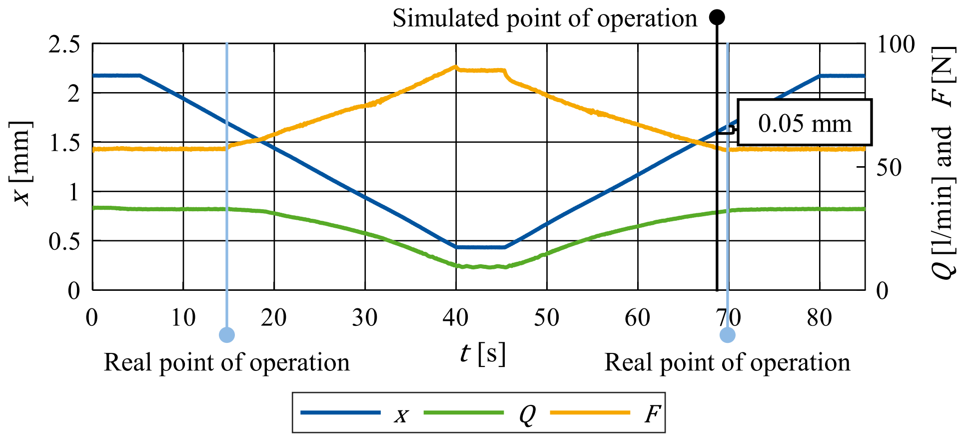

Figure 3.1: Position, force and flow rate curve from a NO valve, flow direction 1-2, tank pressure 30 bar, pressure difference 15 bar

The flow forces should be evaluated during movement, as there is no static friction in this case and the flow force can be calculated from the measurements with and without flow. For this reason, the point 0.05 mm away from the actual operating point is used for the CFD simulation. The actual operating point occurs once during both the closing and opening of the valve. For the simulation, the point at which the actuator extends is used, as there is less possibility of the rod tilting during the extension movement.

For NC valves, it is not possible to determine the actual operating point without further effort. The real operating point is established through a balance of forces between the flow force, spring force and actuator force. The force of the actual solenoid is position-dependent and unknown. For this reason, the actual operating point cannot be read from the measurements and must be assumed. The measurements of all NC valves show a buckle in the flow rate and force curve. This buckle occurs at the point where the valve is opened so far that the smallest cross-section is no longer at the sealing edge. It is assumed that the valves are designed so that point of operation is close to this point where the flow is stable and the flow rate reaches its maximum. This buckle lies at approximately 90 % of the maximum flow rate for all valves, which is why this point is used for simulation.

For validation, all cycles with a tank pressure of 30 bar are used. For nine valves, this results in 164 points that have to be simulated. Once the poppet positions of the operating points to be simulated have been determined, all other required values can be evaluated at these points. These are the flow rate, the flow force as well as the pressures and temperatures upstream and downstream of the test valve. For these variables, an average is calculated for each value using the 50 surrounding values.

3.2. Preliminary Studies

This section details the process and the choices that were made to establish the settings for the geometry, the mesh and the solution which are used for the simulations carried out in this paper. For all simulations Ansys® Fluent® and Fluent® Meshing were used.

3.2.1. Geometry

The simulated geometries belong to industrial poppet valves and were used in their original shape. During the preliminary studies, one geometric variation was tested for their impact on the simulation results. The variation was an extension of the in- and outlet of the manifold by an 80 mm pipe to ensure fully developed flow at the in- and outlet. The pipe influences both the pressure drop and the flow force on the valve. None of the results were implausible so that this variation is to be further investigated based on measurement data.

3.2.2. Mesh

Considering the vast number of simulations that should be conducted, the difference between polyhedron- and tetrahedron-meshes in terms of cell count is significant, facilitating the decision to use polyhedron-meshes. As mentioned in section 2.2.1, unstructured polyhedron-meshes are excessively vulnerable to numerical diffusion for first-order upwind schemes. However, the problem of numerical diffusion is a phenomenon that is limited to first-order upwind discretization schemes. Fluent® uses the second-order upwind scheme as the default discretization for convection terms. Higher order schemes were also tested but did not yield any noticeable effect in the simulation results. In summary, the unstructured polyhedron-mesh with second-order upwind discretization schemes proved to be the best fit for the underlying simulation task. This was also validated by measurements.

The choice of mesh size was an iterative process to find an optimum between desired accuracy and simulation time. A refinement region was placed around a reasonable radius of the poppet, separating the fluid domains with pipe flow and those with, partially turbulent, narrow gap flow. In the next step, both the reference cell size across the entire domain and the refinement factor of the refinement region were iteratively decreased, and increased respectively, until the accuracy of the simulation did not further improve. Said investigations culminated in the establishment of a reference cell size of maximum 0.3 mm and minimum 0.005 mm. The chosen refinement was the factor two. This setup resulted in an average of around 10 million or less cells per simulation.

Another important manipulation of the mesh includes the definition of boundary layers. As mentioned in section 2.2.1, boundary layers are especially crucial for turbulent flows. Ten boundary layers with a growth rate of 1.2 and an aspect ratio of 15 are selected. The first simulations with and without boundary layers showed differences in pressure difference and flow force. In addition, boundary layers increase the number of cells, so the use of boundary layers is to be further investigated based on measurement data.

3.2.3. Solution

The main decision that was to be made in the solution process is the choice of turbulence modeling. An extensive analysis of the Reynolds number across the solution domain yielded the insight that turbulent flow was only present in narrow gaps at high flow rates. Due to the lowest computational costs, RANS simulations were chosen. As mentioned in section 2.2.2 for the turbulence model, the k-ω model is dominant in including near-wall effects. Especially in light of the fact, that boundary layers would not be included in every mesh, it was of vital importance that the turbulence model is able to accurately model near-wall effects in the narrow regions of the fluid domain. For this reason, the widely used k-ω SST (shear stress transport) turbulence model is employed. The alternative of wall functions was also tested by activating the tabulated choice in the near-wall treatment section of Fluent® Setup, however this did not affect the results in a meaningful way.

In the final step of the preliminary investigations, the boundary conditions were examined. Both a flow rate and a pressure boundary condition can be used at the inlet. The investigations showed that the simulations with the flow rate boundary condition converge more quickly, while the pressure boundary condition leads to slight oscillations in the solution. For this reason, the flow rate boundary condition is selected at the inlet. A pressure boundary condition is used at the outlet. A pressure of 500 bar is specified so that positive pressures are always present throughout the solution area during the calculation, and the solution can be calculated more stably. The solver is pressure-based, and all calculations are caried out as steady-state simulations. As convergence criteria, a residual of 0.0005 was used for the outlet flow rate, the pressure difference between inlet and outlet, and the axial flow force acting on the poppet. All CFD simulation parameters specified in the preliminary investigations are summarised in **Table 3.1**. The parameters that are examined in detail in chapter 4 are shown in italics.

Parameter	**Selection**
Simulation environment	Ansys® Fluent®
Mesh type and form	Unstructured polyhedron-mesh
Discretization scheme	Second-order upwind scheme (pressure / momentum / turbulent kinetic energy / specific dissipation rate)
Mesh size	Maximum 0.3 mm; Minimum 0.005 mm
Mesh refinement	In the area of turbulent flow around the poppet with a factor of 2
Type of simulation	RANS
Turbulence model	k-ω SST
Boundary conditions	Inlet: flow rate; Outlet: Pressure 500 bar
Solver	Pressure-based, steady-state
Convergence criteria	Residual of 0.0005 for outlet flow rate, pressure difference, poppet flow force

Boundary layers	*With and without boundary layers, count 10, growth rate 1.2, aspect ratio 15*
Inlet and outlet	*With and without 80 mm pipe*

Table 3.1: Preselected simulation parameters for all simulations

3.3. Methodology and Procedure

This chapter gives a brief overview of the workflow used for the CFD simulations of nine different valve geometries with varying opening widths and boundary conditions. The goal of the simulations is the computation of the pressure loss over the valve and the flow force in axial direction on the poppet. These two quantities are used to validate the CFD simulations with measurement data.

The CAD files for all valves were either provided by the manufacturer or self-created, based on precise measurements. Acute angles in the geometry are to be avoided for a good mesh. Therefore, the geometries were adapted if required. To make the simulations as comparable as possible, the valves are screwed in the manifold with the angle recorded during the measurements [5]. This CAD model is imported to Ansys® with the opening width of the poppet set as a variable. Based on this model, the volume fill is created. The filled area is meshed with the parameters named in Table 3.1.

The CFD simulation uses the poppet position, flow rate and temperatures from the measurements. Before the meshing, the poppet is positioned according to the measured value, and the flow rate is used as an input boundary condition. An ideal Fuchs RENOLIN B 15 VG 46 oil with constant density and viscosity is used in the simulations. The two fluid parameters are determined in advance by a calculation depending on the temperature, and the fluid is modelled as single-phase without cavitation. The temperature used for the calculation is the average of the temperature measured before and after the test valve. After setting the remaining simulation parameters, a so called case-file is exported from Fluent®. The case-file contains the information about the geometry, mesh and all simulation parameters. This file was used to execute the simulations on the High-Performance Computing (HPC) cluster of RWTH Aachen University.

4. RESULTS AND DISCUSSION

A total of 164 points from the measurements of all valves are available for validating the CFD simulations. 86 of these points belong to flow direction 1-2 and 78 to the opposite direction. The 164 points are simulated with four different meshes, but otherwise with the same settings. In the first variant, the geometries are meshed between the male stud connectors using the parameters specified in the preliminary investigations (Table 3.1). In the second variant, an 80 mm inlet and outlet pipe is attached to each of the geometries at the male stud connectors. In variants three and four, the first two variants are each meshed with boundary layers. The parameters listed in Table 3.1 are used for the boundary layers.

In the following, the accuracy of the four different simulation setups will be compared to the measurements. The comparison is carried out individually for the pressure difference Δp and the flow force F_{flow}. Starting with the pressure difference, for a first overview, the simulated values were plotted over the measured values. For both flow directions, the values were evenly distributed around the ideal line and deviate more strongly from the ideal line as the pressure difference increases. A few points in flow direction 2-1 were an exception and had a larger deviation than the rest. These values all came from simulations with boundary layers. A closer look at the points revealed that they all belong to one NC valve. When examining the mesh at this valve, it was found that it has a height of 0.55 mm at the smallest cross-section and that there is only one cell layer between the boundary layers. The lack of an adequate volume mesh between the boundary layers of opposite walls leads to increased deviations. Consequently, there is a systematic error in these simulations. However, all other points indicate that the simulations of the pressure differences are correct and that there is no fundamental error.

To identify which mesh provides the most accurate results, the relative deviation is calculated for each point with **equation 4.1**.

$$relative\ deviation = \left|\frac{simulation - measurement}{measurement}\right| \tag{4.1}$$

The results are illustrated in boxplots in **Figure 4.1**. The boxes mark the range from the lower to the upper quartile. 25 % of all values are below the lower quartile and 25 % of all values are above the upper quartile. The solid line within the box marks the median and the cross marks the mean. All values that are more than 1.5 times of the interquartile range (distance from the upper to the lower quartile) away from the upper or lower quartile are considered outliers. Within the remaining values, the whiskers mark the maximum and minimum values. In flow direction 2-1, the models without boundary layers are the most accurate.

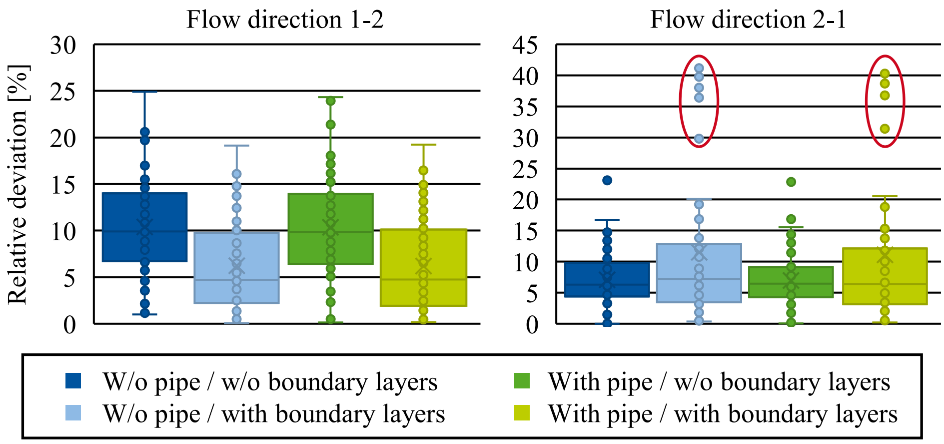

Figure 4.1: Relative deviation of simulated to measured pressure differences for four different meshes in flow direction 1-2 (left) and flow direction 2-1 (right)

The upper quartiles are each below 10 % deviation and the medians are around 6.3 %. The outliers in the models with boundary layers are the same points from the one NC valve already mentioned before. In flow direction 1-2, the simulations with boundary layers are the most accurate. Here, the upper quartiles are approximately 10 % and the medians 4.7 %. In both flow directions, the meshes with and without pipes achieve similar accuracies. In this case, the simulations without pipes are preferable because the mesh is smaller and therefore shorter computing times are possible. The biggest differences are in the simulations with and without boundary layers.

Regarding the accuracy in flow force simulation, **Figure 4.2** shows the simulated flow force plotted over the measured flow force. In contrast to the pressure difference, also negative values are possible for the flow force. The measured values deviate from the ideal line by a similar amount across the entire range and do not converge in a funnel shape. In addition, there is a particularly large number of points at which a flow force close to 0 N was measured, while the simulation yields a larger or smaller value. This occurs in both flow directions, and the areas close to the measured 0 N are marked in red in both diagrams. When calculating the relative values, high percentage deviations would occur at these points, which would reduce the significance of the percentage deviation. For this reason, all points with a measured absolute force of less than 3 N are excluded from the calculation of the relative deviations. One notable feature is the points in flow direction 1-2, which deviate more strongly from the ideal line than the rest. These are also outlined in red and, after verification, could be assigned to the NC valve.

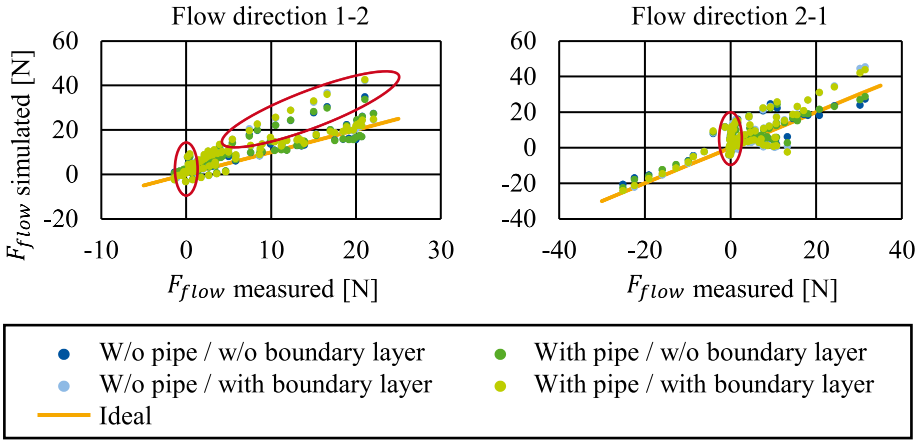

Figure 4.2: Simulated flow force over measured flow force for four different meshes in flow direction 1-2 (left) and flow direction 2-1 (right)

The relative deviation of the flow forces is shown in boxplots in **Figure 4.3**. As already described, all values for which the measured force was less than 3 N are excluded.

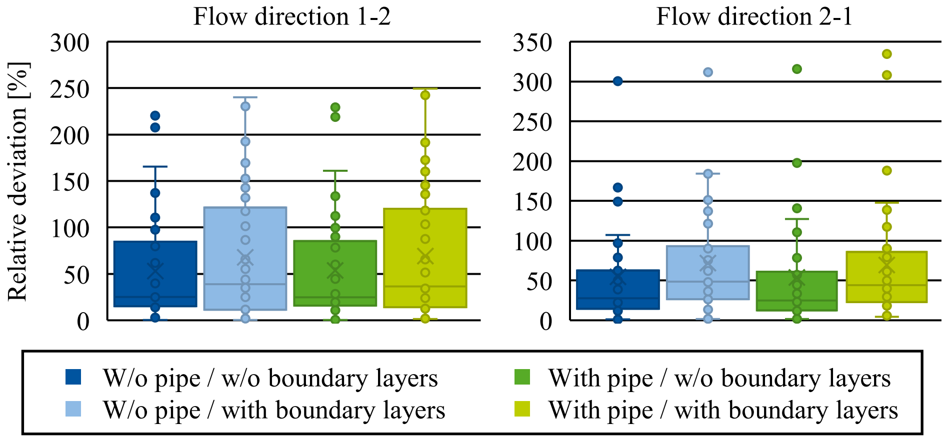

Figure 4.3: Relative deviation of simulated to measured flow forces for four different meshes in flow direction 1-2 (left) and flow direction 2-1 (right)

In flow direction 1-2, 50 of the initial 86 points are still used for the evaluation, and in flow direction 2-1, 44 of the 78 points are still used. The figure shows that the relative deviations in the flow force simulation are significantly greater than in the pressure differences. In both flow directions, the simulations without boundary layers are the most accurate. For these meshes, the upper quartile in flow direction 1-2 is approximately 85 % and the median is approximately 25 %. In the opposite direction, the simulations are more accurate, with the upper quartile at approximately 60 % and the median also at approximately 25 %. This raises the question whether the accuracy of the flow force simulation is sufficient. To clarify this, it is examined which relative deviations occur at which flow forces. It was found that from a measured flow force of 15 N, the relative deviation at each point is less than 26.6 %. High flow forces can therefore be reliably predicted by the simulations.

In summary, in three out of four cases, the mesh without boundary layers was the most accurate. In the case of the pressure difference in direction 1-2, the meshes with boundary layers are more accurate, but the meshes without boundary layers still deliver very good results with an upper quartile of approximately 13 %. For these reasons, a mesh without boundary layers is selected. There are marginal differences between the meshes with and without pipes. Since the mesh without pipes is smaller and the simulations therefore have a shorter calculation time, the mesh without pipes and without boundary layers is ultimately selected for the following simulations which create the database for the prediction models.

Deviations of around 10 % between a CFD simulation and measurements of the real system are currently state of the art in the CFD simulation of pressure differences. This is achieved by the conducted simulations. The accomplished deviations are greater for the flow force, which is why the reason for the deviations should be investigated and discussed at this point.

The first suspicion was a numerical error in the flow force calculation due to different mesh sizes on the poppet surface. For this reason, the poppet geometry and the zone of the mesh refinement were adjusted. Before the adjustment, small shoulders on the poppet led to a locally finer mesh on the surface of the poppet in the pressure compensation area. In addition, the zone of the mesh refinement ended in the pressure compensation bore. During the adjustment, the shoulders were removed in the CAD model and the refinement zone extended, resulting in a mesh with equal size around the poppet.

These changes lead to better matching flow forces, but it is noticeable that the simulations calculate higher values, especially around the range of 0 N measured flow force (Figure 4.2). For this reason, simulations were specifically carried out in which the expected flow force is close to 0 N. This is the case with a low flow rate, which is why all valves were simulated with flow rates from 1 l/min to 5 l/min in 1 l/min increments. The poppet position used was the position that was also used in the simulation with the lowest pressure difference. For two valves, the results show constant flow forces between 6 N and 10 N for these flow rates. These results are implausible and a systematic error in the simulation must be assumed.

Upon closer inspection of the CAD models of the valves, it was noticed that in both models, the manufacturer had also depicted the fits, resulting in clearance between the poppet and the sleeve and thus a gap. This gap was removed for the CFD simulation. To do this, the diameter of the poppet was increased by 0.1 mm so that the poppet and the sleeve overlap. The overlap means that the pressure compensation no longer works, and the poppet is no longer free of forces under static pressure. This problem was solved by matching the poppet diameter with the diameter of the hole in the sleeve exactly.

Another possible reason for the larger percentage deviations in the simulation of the flow forces may be the hysteresis in the flow force [5] in some valves. Previously, the value at the simulated operating point was used as the measured value for comparison. The force hysteresis was not considered. In the following, force hysteresis is taken into account by calculating the mean value of the flow forces between the closing and opening movements and using this as the comparison value.

Overall, the mean average error (MAE) and the mean average percentage error (MAPE) are used to present the final accuracy of the CFD simulation with all the discussed improvements. The two characteristic values are listed for each valve type and flow direction for the pressure difference and flow force in **Table 4.1**. The MAE in the simulation of the pressure difference is between 0.7 bar and 1.7 bar, depending on the valve type and flow direction. This corresponds to average percentage errors of 5.5 % to 11.1 %. The accuracies achieved are mostly below this value and, in the case of NC valves in flow direction 1-2, just above it. When simulating the flow forces, there are greater deviations from the measured values. The average deviation is between 2.8 N and 3.6 N. In percentage terms, this results in a deviation of between 36.6 % and 67.3 %. Bordovsky [7] obtains a $MAPE$ of 32 % with a simulation optimized for one valve. So, the $MAPE$ achieved with general simulation settings applied on nine different geometries can be rated as good. Despite the higher deviations, the trends in the flow force simulation are correct. This means that values in this accuracy range are also suitable for setting up a prediction model.

Δp	NO 1-2	NO 2-1	NC 1-2	NC 2-1	F_{flow}	NO 1-2	NO 2-1	NC 1-2	NC 2-1
MAE [bar]	1.1	0.7	1.7	0.7	MAE [N]	3.5	3.4	2.8	3.6
$MAPE$ [%]	8.8	6	11.1	5.5	$MAPE$ [%]	38.4	58.3	67.3	36.6

Table 4.1: MAE and $MAPE$ of simulated to measured values of pressure difference and flow force divided according to valve type and flow direction

In summary, it can be said that CFD simulations have potential as a database for prediction models. The achieved accuracies are satisfactory. For an individual valve, the simulation parameters could be further improved. Since the results originate from nine different valves, the CFD simulation parameters for the various geometries of this type and size of 2/2 directional poppet valves are validated. It can be assumed that simulations of other geometries using the same CFD simulation parameters will achieve similar accuracies.

5. CONCLUSION AND OUTLOOK

In this paper generally applicable CFD simulation parameters for 2/2 directional poppet valves were acquired. In extensive preliminary investigations, several simulation parameters, such as a polyhedron-mesh with a maximum size of 0.3 mm, were selected. An overall number of 164 points, generated from measurement data, were simulated with four different meshes. The mesh without an additional pipe and without boundary layers turned out to be the best compromise between accuracy and computing efficiency. The simulation of the pressure difference has a mean deviation of 7.9 % to measured data. The flow force simulation has a mean deviation of 50.2 %, but the trends in the flow force simulation are correct. This makes CFD simulations with the presented parameters suitable as a database for pressure drop and flow force prediction models of 2/2 directional poppet valves. The CFD simulations are particularly reliable for the pressure drop and for flow forces above 15 N. In future work, the determined simulation parameters can be applied to a variety of geometries and thus create a database for prediction models of 2/2 directional poppet valves. Before using the determined parameters in CFD simulations of other valves, the parameters must be validated separately.

6. ACKNOWLEDGEMENTS

The IGF research project 01IF22852N of the research association Forschungskuratorium Maschinenbau e. V. – FKM, Lyoner Straße 18, 60528 Frankfurt am Main was supported from the budget of the Federal Ministry of Economic Affairs and Climate Action through the DLR within the scope of a program to support industrial community research and development (IGF) based on a decision of the German Bundestag.

Computations were performed with computing resources granted by RWTH Aachen University under project rwth1768.

7. REFERENCES

[1] Deloitte: 'Wachstumsmotor Maschinenbau - Vier Szenarien für eine erfolgreiche Zukunft in 2030', 2021.

[2] PwC: 'Maschinenbau-Barometer - Ausblick 2026', 2025.

[3] Yuan, Q., Singh, S. et al. 'Flow Forces Investigation through Computational Fluid Dynamics and Experimental Study', 9th International Fluid Power Conference (9th IFK), pp. 100–109, 2014.

[4] Bordovský, P. 'Evaluation of Steady-State Flow Forces in Spool Valves', Dissertation, Aachen, 2018.

[5] Rothhardt, T., Schmitz, K. 'First Steps Towards Model-Based Valve Design: Measuring Pressure Drop and Flow Forces of Industrial 2/2 Directional Poppet Valves', The 19th Scandinavian International Conference on Fluid Power, SICFP'25, pp. 424–435, 2025. DOI: 10.13052/rp-9788743808251A31.

[6] Vaughan, N. D., Johnston, D. N., Edge, K. A. 'Numerical Simulation of Fluid Flow in Poppet Valves', Proceedings of the Institution of Mechanical Engineers, Part C: Journal of Mechanical Engineering Science, Vol. 206, Nr. 2, pp. 119–127, 1992. DOI: 10.1243/PIME_PROC_1992_206_105_02.

[7] Bordovský, P., Schmitz, K., Murrenhoff, H. 'CFD Simulation and Measurement of Flow Forces Acting on a Spool Valve', 10th International Fluid Power Conference, pp. 473–484, 2016.

[8] Zong, C., Zheng, F. et al. 'Computational Fluid Dynamics Analysis of the Flow Force Exerted on the Disk of a Direct-Operated Pressure Safety Valve in Energy System', Journal of Pressure Vessel Technology, Vol. 142, Nr. 1, 2020. DOI: 10.1115/1.4045131.

[9] Domagala, M., Fabis-Domagala, J. 'A Review of the CFD Method in the Modeling of Flow Forces', Energies, Vol. 16, Nr. 16, 2023. DOI: 10.3390/en16166059.

[10] Bernad, S. I., Susan-Resiga, R. 'Numerical Model for Cavitational Flow in Hydraulic Poppet Valves', Modelling and Simulation in Engineering, Vol. 2012, pp. 1–10, 2012. DOI: 10.1155/2012/742162.

[11] Hao, Q., Wu, W., Tian, G. 'Study on reducing both flow force and cavitation in poppet valves', Proceedings of the Institution of Mechanical Engineers, Part C:

Journal of Mechanical Engineering Science, Vol. 236, Nr. 23, pp. 11160–11179, 2022. DOI: 10.1177/09544062221110729.

[12] Simic, M., Herakovic, N. 'CFD Simulation and Optimization of Hydraulic ON/OFF Valve for Small Volume Flow', 8th International Fluid Power Conference, 2012.

[13] Simic, M., Herakovic, N. 'Reduction of the flow forces in a small hydraulic seat valve as alternative approach to improve the valve characteristics', Energy Conversion and Management, Vol. 89, pp. 708–718, 2015. DOI: 10.1016/j.enconman.2014.10.037.

[14] Xie, H., Tan, L. et al. 'Research on Influence of Different types of Orifice on Axial Steady-state Flow Force in Cartridge Proportional Valve', International Journal of Fluid Power, 2019. DOI: 10.13052/ijfp1439-9776.2021.

[15] Liu, J., Li, R. et al. 'Flow force research and structure improvement of cartridge valve core based on CFD method', Heliyon, Vol. 8, Nr. 11, e11700, 2022. DOI: 10.1016/j.heliyon.2022.e11700.

[16] Rundo, M., Altare, G. 'Comparison of Analytical and Numerical Methods for the Evaluation of the Flow Forces in Conical Poppet Valves with Direct and Reverse Flow', Energy Procedia, Vol. 126, pp. 1107–1114, 2017. DOI: 10.1016/j.egypro.2017.08.261.

[17] Roemer, D. B., Johansen, P. et al. 'Modeling of movement-induced and flow-induced fluid forces in fast switching valves', 2015 International Conference on Fluid Power and Mechatronics (FPM), pp. 978–983, 2015. DOI: 10.1109/FPM.2015.7337257.

[18] Gomez, I., Gonzalez-Mancera, A. et al. 'Analysis of the Design of a Poppet Valve by Transitory Simulation', Energies, Vol. 12, Nr. 5, pp. 889, 2019. DOI: 10.3390/en12050889.

[19] Finesso, R., Rundo, M. 'Numerical and Experimental Investigation on a Conical Poppet Relief Valve with Flow Force Compensation', International Journal of Fluid Power, Vol. 18, Nr. 2, pp. 111–122, 2017. DOI: 10.1080/14399776.2017.1296740.

[20] Hirose, N., Masuda, S. et al. 'Flow Patterns and Hysteresis Characteristic of a Poppet Valve', JFPS International Journal of Fluid Power System, Vol. 15, Nr. 2, pp. 53–61, 2022. DOI: 10.5739/jfpsij.15.53.

[21] Johnston, D. N., Edge, K. A., Vaughan, N. D. 'Experimental investigation of flow and force characteristics of hydraulic poppet and disc valves', Proceedings of the Institution of Mechanical Engineers, Nr. 205, pp. 161–171, 1991.

[22] Ferziger, J. H., Perić, M., Street, R. L. 'Computational Methods for Fluid Dynamics', Springer International Publishing, Cham, 2020. DOI: 10.1007/978-3-319-99693-6.

[23] Vinchurkar, S., Longest, P. W. 'Evaluation of hexahedral, prismatic and hybrid mesh styles for simulating respiratory aerosol dynamics', Computers & Fluids, Vol. 37, Nr. 3, pp. 317–331, 2008. DOI: 10.1016/j.compfluid.2007.05.001.

[24] Lintermann, A. 'Computational Meshing for CFD Simulations', 2021. DOI: 10.1007/978-981-15-6716-2_6.

[25] Ansys, Inc. 'Ansys Fluent Theory Guide - 2025R2', https://ansyshelp.ansys.com, 2025.

Biographies

Timo Rothhardt received the bachelor's degree in mechanical engineering from RWTH Aachen University in 2020 and the master's degree in product development in 2023. He is currently working at RWTH Aachen as scientific staff in the Institute for Fluid Power Drives and Systems (ifas). As part of the team high-performance components, his research areas include valves, CFD simulation, design of experiments and machine learning.

Prof. Katharina Schmitz studied mechanical and chemical engineering at RWTH Aachen University and Carnegie Mellon University, Pittsburgh (USA) and graduated 2015 as Dr.-Ing. at RWTH Aachen University. Since 2018, she is full professor at RWTH Aachen University and director of the Institute for Fluid Power Drives and Systems (ifas). In addition, she is Vice Dean of the Faculty for Mechanical Engineering at RWTH Aachen, a position she holds since 2020. Prof. Schmitz's awards and honors include several best paper awards and 2023 IMechE Joseph Bramah Medal award.